

1 INTRODUCTION

Rheology is a study of deformation and flow of matter. Of special interest are the materials which do not follow the Newton's law of viscosity. Newtonian materials flow in the usual way, whereas non-Newtonian materials flow in an unusual way, exhibiting various interesting and peculiar flow phenomena. Rheology therefore is a very interdisciplinary study: Research of non-Newtonian fluids is carried out, for example, in paint and lacquer industry, oil drilling, food industry, pharmacology, and polymer processing. Polymers consist of long chain macromolecules, which largely determine their non-Newtonian flow behavior. They are further defined as viscoelastic materials, which means that their behavior is somewhere between that of elastic solids and viscous fluids.

In order to understand and manage the melt processing of polymers one needs to understand and be able to quantify the rheological phenomena occurring in processing flows. Rheology plays a significant role in determining melt processability of polymers, as well as physical properties of the processed end-products. Despite that, industrial polymer processors often take shortcuts in rheological characterization. This is probably partly due to the tedious nature of experiments or expensive characterization equipment needed, partly because of a belief that some phenomena, such as the ones discussed in this study, do not have a great importance in predicting the flow behavior or interpretation of the results.

For successful production set up the plastic processors should have a solid understanding of the properties and behavior of the used polymer resins. A consistent data bank including the rheological properties of polymers would benefit the plastic processors who will, using their existing knowledge and the aid of the documented data, tailor the process parameters to suit the properties of each polymer for manufacturing flawless products. Knowledge on rheological behavior of polymers is needed for finding the optimal melt processing conditions, such as temperature and rate of flow, and for estimating the required machine capacity. In addition, rheological data provides essential input for process simulation, which is increasingly adapted as an important part of new process setup and product design. Simulation software is used to enhance the productivity, quality, turnaround times and resource utilization in polymer processing. However, the feasibility of simulation software is strongly dependent on the expertise of the user, the accuracy of the material data and models in its database, and on the understanding of the material behavior. Rheological properties of polymer melts are of particular importance in flow modeling.

Hundreds of different grades of commercial polymers are on the market, and they can have widely varying processing characteristics even within the same base polymer. At present the requirements for manufacturing processes are higher than ever; increasingly finer details and functionalities are implemented in plastic parts, such as combinations of different materials or integration of special functions. At the same time many technical plastic products face very stringent quality requirements such as high strength, small tolerances, dimensional stability, and surface smoothness. Not only the quality of the product, but also the cost effectiveness of the whole process, is

2 OVERVIEW TO POLYMER RHEOLOGY

2.1 Basic flow characteristics of polymers

Factors related to the molecular structure of polymers set challenges to their successful processing; unlike metals or ceramics, polymeric materials consist of very long chain-like macromolecules. This leads to rather complex rheological behavior in the molten state. The relationship between elastic shear stress τ_e and strain γ for fully *elastic* materials, such as metals, is determined by Hooke's law.

$$\tau_e = G\gamma \quad (1)$$

For pure *viscous* liquids – such as water, oil, or syrup – deformation is time-dependent, and the relationship between the viscous shear stress τ_v and strain *rate* $\dot{\gamma}$ is determined by Newton's law.

$$\tau_v = \eta\dot{\gamma} \quad (2)$$

For *Newtonian* fluids viscosity η is a material constant and not dependent of the rate of deformation. For fully elastic materials the strain is directly proportional to the stress with a factor called shear modulus G (for shear) or Young's modulus E (for tension), and the elastic energy is stored in the substance upon deforming it. Thus the strain is totally recoverable after permitting the material to return to its undeformed equilibrium state, provided that the limit of plastic deformation was not exceeded in loading. For pure viscous materials all the energy is dissipated in the continuous deformation, thus the amount of recoverable strain is zero. The deformation follows the applied stress with delay¹.

The properties of polymer melts lie somewhere between Hookean and Newtonian materials, thus they are *viscoelastic* liquids by nature. Cross-linked rubbers have properties closer to the elastic materials and they are often referred to as viscoelastic solids. Viscoelasticity makes the materials' response to stress-strain behavior time dependent and their deformation partially reversible. Polymer melts are further defined as *non-Newtonian* fluids: their viscosity is not constant, thus the relationship between deformation rate and stress is not linear. The reasons for non-Newtonian behavior can be found in the molecular structure: Polymers consist of long molecules that entangle with each other, forming several flexible, reversible "joints". These enable different conformations of the molecules by a rotation along the backbone and cause the elastic behavior of polymer melts. The chains can also move with respect to each other by a crawling kind of movement called reptation. These rotation and reptation occurring above the glass transition temperature of the polymer are called Brownian motions, and they tend to return the molecules towards the equilibrium, i.e., to the energetically most preferable state, after being oriented by applying deforming stress. This will not,

however, occur immediately after removing the stress but within a certain relaxation time, dependent on the molecular characteristics of the polymer¹.

From the polymer processing point of view, among all non-Newtonian phenomena the most important one for polymer melts is their common *shear thinning* characteristic, which means that their viscosity decreases as a function of shear rate. This occurs due to orientation and disentanglement of the entangled macromolecules in the melt when a certain critical shear rate (limit of the linear viscoelasticity; change from the zero-shear viscosity to shear thinning behavior) is exceeded. Shear thinning is actually the property that ultimately enables many of the melt processing techniques of polymers¹.

2.1.1 Linear viscoelasticity and mechanical models

When very small deformation is applied to the polymer melt, or when the deformation rate is very slow, the molecules have enough time to relax through the Brownian motion and the polymer structure remains unaltered; the entangled and coiled state of the molecules is not disturbed. The deformation is said to be in the *linear viscoelastic range*. For characterizing the inherent material properties in rheological experiments, it is essential that the measurements are done in the linear viscoelastic range, i.e. the deformation is kept small enough. The relaxation of the molecules is described by relaxation modulus G . According to the Boltzmann superposition principle, in the linear viscoelastic region the response of a material to series of step strains is a sum of the responses of the each step (total stress $\tau(t)$ is the sum of stresses generated at each step from time t' to t . $\dot{\gamma}$ is the shear rate):

$$\tau(t) = \int_{-\infty}^t G(t - t') \dot{\gamma}(t') dt' \quad (3)$$

The responses of viscoelastic materials to applied stress or strain can be modeled with the aid of mechanical spring-dashpot analogies. The dashpot describes the viscous, and the spring the elastic response to the applied load or deformation. The dashpot represents the time dependence and relates to the characteristic relaxation time of a material, the time the molecule needs to return to the equilibrium state after deformation¹.

The Maxwell model consists of a dashpot and spring in series (Figure 1a) and is a simplest model to describe the behavior of viscoelastic liquids. As can be figured from this setting, the dashpot allows for indefinite deformation; for a viscoelastic fluid no limiting cross-links exist, unlike in viscoelastic solids. The Maxwell model describes the stress relaxation of a polymer: decay of the stress at a constant, pre-defined strain. However, the one-element Maxwell model alone is not able to describe the stress relaxation behavior of true viscoelastic liquids, as they are always more complex systems consisting of distribution of molecule chains lengths. The generalized Maxwell model (Figure 1b) consists of series of n Maxwell elements, and gives a closer-to-reality picture of the behavior of viscoelastic fluids, such as polymer melts above their glass transition and melting temperatures. It describes the relaxation time spectrum of a polymer; each length of molecule has a characteristic relaxation time and each element represents one of them.

The Kelvin model (also called the Kelvin-Voigt or Voigt model) combines one dashpot and one spring in parallel (Figure 1c), modeling the behavior of viscoelastic solids, such as cross-linked rubbers. This model describes the *creep* and *creep recovery* behavior; constant loading condition causes a “creeping” – time dependent strain deformation – of the material. Similarly, the strain recovery after stress removal does not occur instantaneously but depends on the material’s characteristic time. The Kelvin model allows for a completely recoverable strain, thus it does not describe the creep

recovery behavior of molten thermoplastics correctly. For modeling the creep of polymer melts, at least one dashpot element has to be added in series with the Kelvin model in order to model the non-recoverable portion of strain. In a creep test a constant stress is applied to the sample, and the following deformation strain is recorded. When the applied stress is removed, strain recovery is observed: The material returns partially to the original, undeformed state^{2,3}.

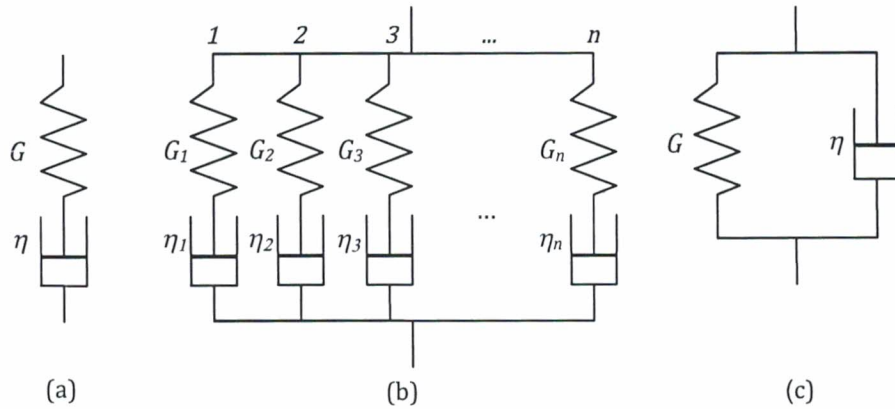


Figure 1. Representation of the Maxwell model (a), the generalized Maxwell model (b), and the Kelvin model (c)

The behavior of real polymer systems in creep or stress relaxation can be modeled using the different combinations of mechanical model analogies presented above, nevertheless, they do not describe the structure of viscoelastic solids or liquids physically, neither give quantitative information of viscoelasticity. Creep/creep recovery, stress relaxation, and *small amplitude oscillatory shear* (SAOS) experiments are used to characterize the linear viscoelastic properties of polymers. SAOS involves dynamic load of the material at small pre-defined strain amplitude at changing frequency. In oscillatory shear the deformation is sinusoidal – provided that the deformation is in the linear viscoelastic region – and the viscoelasticity manifests itself as a phase lag between the applied stress and the strain (Figure 2). The phase lag between stress and strain is expressed as the phase angle δ .

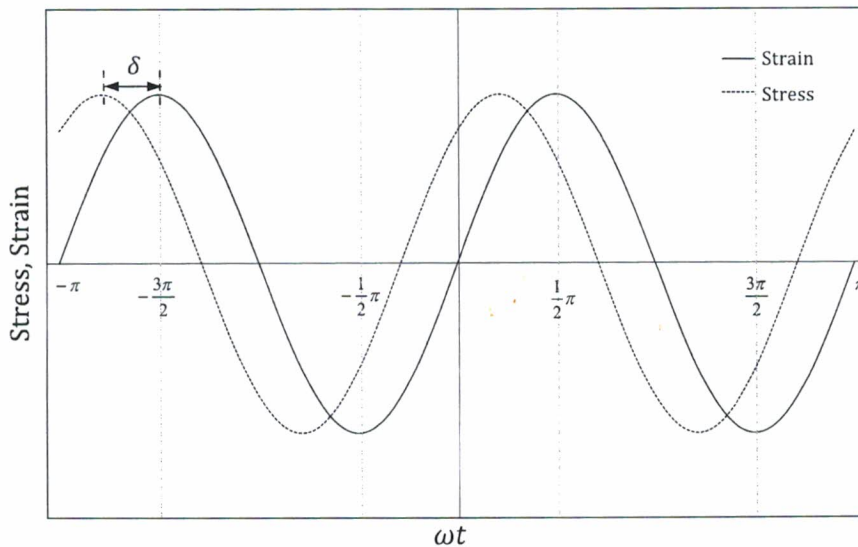


Figure 2. Sinusoidal forms of stress and strain for a viscoelastic substance.

The strain function has the form

$$\gamma = \gamma_0 \sin \omega t \quad (4)$$

γ_0 = strain amplitude and ω = angular frequency. Correspondingly, the stress is

$$\tau = \tau_0 \sin(\omega t + \delta) \quad (5)$$

Stress consists of in-phase (τ') and out-of-phase (τ'') components, from which the first one relates to the elastic and the latter one to the viscous part of the response to applied strain:

$$\tau = \tau' + \tau'' = \tau'_0 \sin \omega t + \tau''_0 \cos \omega t \quad (6)$$

The out-of-phase component of the stress is in phase with the strain rate, which is the time derivative of the small-amplitude strain:

$$\dot{\gamma} = \frac{d\gamma}{dt} = \dot{\gamma}_0 \cos \omega t \quad (7)$$

where $\dot{\gamma}_0$ = strain rate amplitude. The viscoelastic moduli: *storage modulus* G' representing the elastic part i.e. the amount of energy stored in the material and the *loss modulus* G'' representing the viscous part, i.e. the energy dissipated in the deformation are:

$$G' = \frac{\tau'_0}{\gamma_0} \quad G'' = \frac{\tau''_0}{\gamma_0} \quad (8)$$

The relation between the viscoelastic moduli is called the loss factor:

$$\tan \delta = \frac{G''}{G'} \quad (9)$$

The relation between the moduli and frequency can be expressed as magnitude of *complex viscosity* (from this point onwards simply 'complex viscosity') consisting of the viscous and elastic parts:

$$|\eta^*| = \sqrt{(\eta'^2 + \eta''^2)} = \sqrt{\left[\left(\frac{G'}{\omega}\right)^2 + \left(\frac{G''}{\omega}\right)^2\right]} = \frac{|G^*|}{\omega} \quad (10)$$

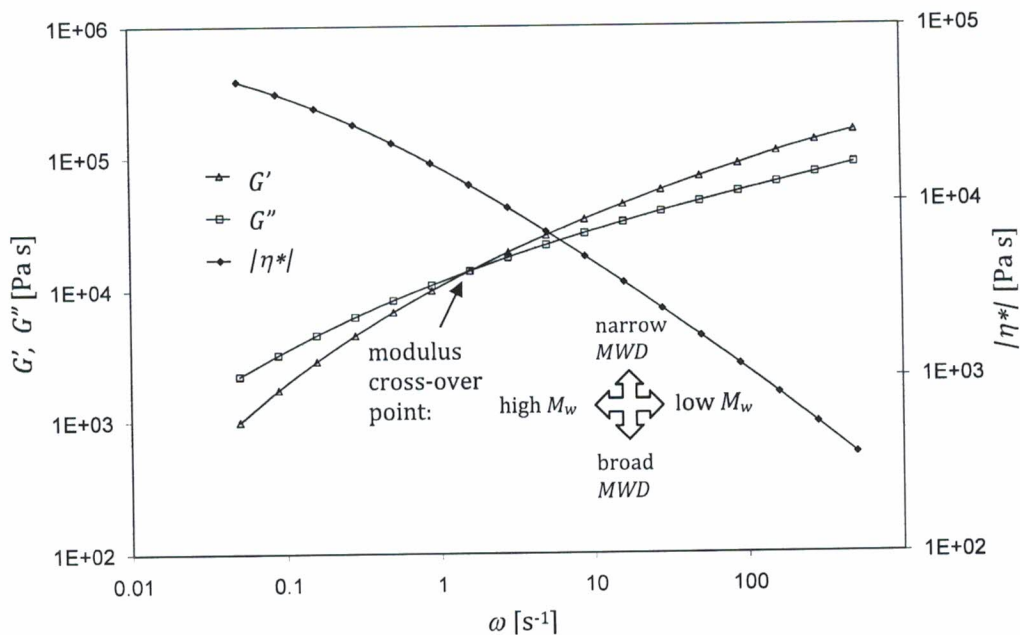


Figure 3. Result curves from a typical SAOS test. Location of the cross-over point of G' and G'' gives information about the molecular weight and molecular weight distribution.

In SAOS tests the dynamic moduli vs. frequency are determined from the stress vs. strain response of the material. At low frequencies the loss modulus is higher, thus the material behaves more like a liquid, while at high frequencies the storage modulus, and thus the solid-like behavior, dominates. The cross-over point of the curves, where $G'=G''$, gives an indication of the average molecular weight (M_w) and breadth of the molecular weight distribution (MWD) of polymers as shown in Figure 3. *Long-chain branching* (LCB), which is present for example in the molecular structure of low-density polyethylene, increases the elasticity of the melt and shifts the modulus cross-over point to the left².

2.1.2 Non-linear viscoelasticity

When the deformation amplitude or rate is increased, the entanglements of molecule chains start to reorganize and orientate along the flow. This means that the deformation exceeds the limit of linear viscoelasticity and the melt structure is destroyed. The material response becomes dependent on the rate, kinematics and magnitude of deformation, and the load is said to be in the *non-linear* region. In the polymer melt processing the extent of deformation is not small and slow but occurs in the non-linear region, and in order to get information about the melt behavior in processing flows, rheological measurements in the non-linear viscoelastic region are important.

Description of the material response in the non-linear world gets more complex because of the need to include deformation and deformation rate into consideration. In other words, a property, such as shear viscosity, is always dependent on the shear rate, and those measured at different strain rates are not comparable to each other. Moreover, one has to consider the deformation kinematics; thus the extensional behavior of a material cannot be derived from shear experiments or vice versa. The real-world phenomena, such as those occurring in plastics processing, most often involve rapid and large deformations, thus the need for knowledge of non-linear behavior is clear.

Newtonian fluid flow exhibits only a stress component in the flow direction (x_1 , see Figure 4 on page 11), whereas in polymer melts also normal stresses, that is, stress components in the parallel directions (Figure 4, x_2 and x_3), are found due to the fluids' viscoelastic nature. As polymer melts in normal cases are considered incompressible, the normal stresses are isotropic, and do not cause any deformation. Therefore the absolute normal stress values have no rheological significance. However, the difference between the normal stresses acting in different directions causes deformation and is significant from the rheological point of view. For simple shear flow normal stresses are thus expressed as normal stress differences: the difference between the 1st and 2nd diagonal component (1st normal stress difference N_1) and the difference between the 2nd and 3rd diagonal component (2nd normal stress difference N_2) in the tensor notation for the shear stress¹.

At the steady-state of a start-up flow or creep flow the non-linear rheological behavior of the polymer can be fully described with the aid of three viscometric functions that depend on shear rate; viscosity η , 1st normal stress coefficient ψ_1 and 2nd normal stress coefficient ψ_2 :

$$\eta(\dot{\gamma}) = \frac{\tau_{21}}{\dot{\gamma}_0} \quad (11)$$

$$\psi_1(\dot{\gamma}) = \frac{\tau_{11} - \tau_{22}}{\dot{\gamma}_0^2} \quad (12)$$

$$\psi_2(\dot{\gamma}) = \frac{\tau_{22} - \tau_{33}}{\dot{\gamma}_0^2} \quad (13)$$

where τ_{11} , τ_{22} , and τ_{33} are the diagonal components of the stress tensor. $\psi_1(\dot{\gamma})$ is usually regarded as positive-signed, whereas $\psi_2(\dot{\gamma})$ has an opposite sign and its magnitude is only a fraction of that for $\psi_1(\dot{\gamma})$. Most commonly in determining the polymer properties for processing purposes, the quantity of major interest is the shear viscosity as a function of shear rate. In fact, the determination of normal stress differences is much more complicated than that of $\eta(\dot{\gamma})$, and lot less is known about them. However, the normal stress coefficients give important information about the viscoelastic properties of the melt and are, together with other rheological measures, significant in characterizing molecular structures: η_0 and $\psi_1(\dot{\gamma})$ are both proportional to the molecular weight of the polymer^{1,2,3}. Moreover, observing changes in normal stress differences during the step-strain measurements by cone-plate and plate-plate experiments gives indications about edge flow instabilities⁴, and has also been related to the instabilities occurring in extruding flows, for example in capillary rheometry⁵.

2.1.3 Cox-Merz rule

An empirical rule found out by Cox and Merz⁶ creates a link between the linear and non-linear quantities. If the Cox-Merz rule is applicable, the complex viscosity from SAOS test and steady-shear viscosity can be combined so that

$$\eta(\dot{\gamma}) = |\eta^*(\omega)|, \text{ when } \dot{\gamma} = \omega \quad (14)$$

Originally, the rule was found to hold for two different polystyrenes between dynamic data and capillary rheometry data. In capillary rheometry, issues such as entrance pressure drop and pressure effects can impair the compatibility of data, thus the applicability of the rule depends on the polymer in question and must in unclear cases be separately checked. The two before-mentioned factors naturally do not affect the

compatibility if dynamic data is combined with steady-shear data from a rotational rheometer.

The advantage of applying the Cox-Merz rule is the smaller number of experiments needed for characterization: both linear viscoelastic characteristics and non-linear flow properties can be extracted from same measurements. Moreover, the maximum shear rate range of the rotational rheometer is 'extended': in the steady step-shear mode the maximum rate due to arising edge fracture (see Chapter 3.1) is about 10 s^{-1} , but in the dynamic mode rheometers can typically be operated at up to 100 Hz, which corresponds to an angular frequency of 628 s^{-1} .

2.1.4 Temperature dependence and time-temperature superposition

Polymer molecules constantly exhibit a so called Brownian motion; they can move past each other, rotate and reptate in large number of possible conformations due to their length and flexibility. The Brownian motion of an individual chain is largely inhibited by the other molecules surrounding it. This is also referred to as entanglements of the chains, although the chains do not necessarily need to be looped together; the chains packed closely together in the melt just do not have space, thus they are inhibiting each others' motions². When the temperature of the melt is increased, the Brownian motions of the chains augment and the *free volume* around the polymer chains increases. Increased free volume means easier flow, and decreased viscosity⁷.

The extent to which the viscoelastic properties are dependent on temperature is traced back to the molecular structure of the polymer chains: The more complex the structure – i.e. the more branches, large pendant groups, and ring structures it has – the stronger the effect of temperature on the viscosity, since the greater is then the relative change in the free volume as a function of temperature⁷. In order to make the polymer melt to flow, the chain segments must have enough free space around them and there must be enough thermal energy to overcome the motion-inhibiting barriers, such as rotation around covalent bonds¹.

If the viscoelastic functions of a polymer measured at different temperatures can be shifted by a single shift factor to one, selected reference temperature to form a *master curve* with a good superposition, the material is *thermo-rheologically simple*, meaning that all the relaxation times have the same temperature dependence. Quantities including a stress component, such as the storage and loss moduli, are shifted by multiplying with a *vertical shift factor* b_T and the quantities including time, such as frequency or shear rate, with *horizontal shift factor* a_T . This procedure is called the *time-temperature superposition* (TTS). If TTS is valid and shift factors can be used to create a master curve from linear viscoelastic data, the same shift factors should in principle be also applicable for shifting non-linear data, e.g. viscosity as a function of shear rate. When the quantity to be shifted includes both time and stress, like viscosity does, both horizontal and vertical shift factors should be applied: the viscosity is shifted by multiplying with the factor b_T/a_T to yield the 'reduced' viscosity η_r

$$\eta_r = \frac{\eta(\dot{\gamma}, T) b_T}{a_T} \quad (15)$$

and the reduced shear rate is obtained by shifting $\dot{\gamma}$ with a_T

$$\dot{\gamma}_r = a_T \dot{\gamma} \quad (16)$$

The vertical shift factor is given as

$$b_T = \frac{T_{ref} \rho_{ref}}{T \rho} \quad (17)$$

with T = temperature and ρ = density, and T_{ref} and ρ_{ref} , respectively are the reference temperature and pressure. However, the vertical shift factor b_T is relatively insensitive to temperature, and often taken to be unity. Then the viscosity can be shifted by the horizontal shift factor only, and has the form

$$\eta_r = \frac{\eta(\dot{\gamma}, T)}{a_T} \quad (18)$$

The horizontal temperature shift factor at $T \leq T_g + 100$ K can be described according to Williams, Landel and Ferry (the WLF equation)⁸ as

$$\log a_T = -\frac{C_1(T - T_{ref})}{C_2 + (T - T_{ref})} \quad (19)$$

with C_1 and C_2 as fitting parameters. When $T_{ref} = T_g$ these parameters have been observed to have universal constant values $C_1 = 17.44$ and $C_2 = 51.6$ K, based on a fitting on a large number of polymers. The more accurate approximation with WLF equation was found when T_{ref} was not treated as a fixed parameter but allowed to be adjusted being ~ 50 K above the glass transition temperature. This was accomplished with the constants $C_1 = 8.86$ and $C_2 = 101.6$ K⁸. At temperatures higher than $T_g + 100$ K the free volume is no longer a limiting factor, but the energy barriers resisting the flow become significant. Then the temperature dependence is better expressed by the Arrhenius equation⁷:

$$a_T = \exp\left[\frac{E}{R}\left(\frac{1}{T} - \frac{1}{T_{ref}}\right)\right] \quad (20)$$

where E is the activation energy of flow and R = ideal gas constant = 8.314 J/mol·K. The activation energy of flow gives an indication about the molecular structure and chain branching⁹: typically polymers with LCB structures have higher E than the linear ones.

The master curve presentation is sometimes used even when a material shows thermo-rheological complexity. In such cases no information about the molecular features of the polymer can be achieved from the master curves, however, they show the general trend of rheological behavior over a wide range of deformation¹⁰.

2.1.5 Pressure dependence

Generally fluids, such as polymer melts, are considered incompressible. Nevertheless, at high hydrostatic pressures that can occur in melt processing, they do exhibit some compressibility. Therefore pressure also has an effect on viscosity, albeit not nearly as strong as temperature. The pressure dependence of viscosity of polymer melts has a practical significance in high-pressure processes, such as injection molding, where pressure frequently exceeds 100 MPa. In an analogous manner to the temperature dependence, viscosity as a function of pressure obeys exponential behavior, but with an inverse effect: the free volume between the molecules decreases when the pressure increases, and thus the Brownian motions of the chains are more inhibited. Therefore an increase in pressure also increases viscosity. A common way to describe the pressure effect on viscosity is to use the Barus equation

$$\eta_{0,p} = \eta_{0,np} e^{\beta p} \quad (21)$$

where and $\eta_{0,np}$ = zero-shear viscosity at normal (atmospheric) pressure, p = pressure and β = material-characteristic pressure coefficient. The pressure shift factor is thus

$$a_p = e^{\beta p} \quad (22)$$

In the vicinity of the T_g the effect of pressure, as also the effect of temperature, is larger than at higher temperatures¹¹. Pressure induced crystallization can also occur at elevated pressures, causing solidification above the T_m of atmospheric pressure, and this naturally causes a strong increase in melt viscosity¹.

According to Cogswell¹² the pressure dependence can be expressed in terms of equivalent change in temperature as a pressure-temperature coefficient $(dT/dp)_\eta$ which has an average value of -5×10^{-7} K/Pa meaning that an increase of pressure by 100 MPa would correspond to a decrease of temperature by 50 K. The exact value of the coefficient varies depending on the polymer in question in the same way as for the temperature dependence.

2.2 Viscometric Flows

Two types of flows are commonly studied for non-Newtonian fluids: *simple shear* and *simple elongational (extensional) flow*. Shear flow takes place in various industrial processes, and is also the easiest flow type to generate in laboratory circumstances. Simple shear is uniform flow: each fluid element on a same stream line undergoes exactly the same deformation and the distance between them remains unchanged (Figure 4).

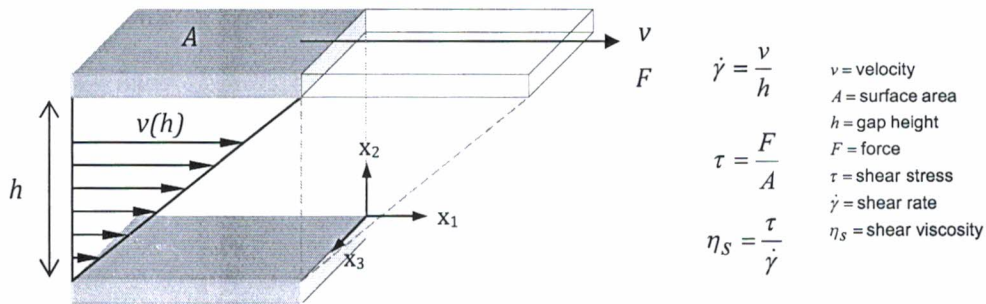


Figure 4. Representation of velocity fields in simple shear flow

The term *viscometric flow* embodies both the uniform, simple shear flow and the non-uniform shear flows that occur in rheometry and common processes, and where the fluid behavior can be governed by three functions; viscosity, first and second normal stress coefficients. Viscometric flows can be divided into *drag flow* and *pressure driven flow (Poiseuille flow)* according to the way the shear is created: in drag flow shearing is generated between two surfaces, moving the one while keeping the other stationary, as for simple shear in Figure 4. In pressure-driven flow, shearing occurs due to the pressure gradient in a closed channel. *Tube or capillary flow* is the pressure-driven flow most commonly used to measure the shear viscosity of polymers. This type of flow occurs in circular channels and slits and can be described as a telescope-like behavior of fluid elements, where the velocity at the centerline of the flow is at highest and zero next to the wall, assuming that no slip occurs between the wall and the melt (Figure 5). Correspondingly the shear rate is at highest on the wall, and zero on the centerline^{1,3}.



Figure 5. Representation of velocity fields in pressure-driven tube and slit flow.

2.3 Extensional Flows

Besides shear flow, melt can experience extensional (or elongational) flow during processing. This means that the material undergoes stretching along the streamlines as a consequence of extensional deformation and the distance between particles on the same streamline changes. The simplest extensional flow type is *uniaxial extension*: stretching of the material in one direction causes compression in the other two directions. In *biaxial extension* the velocity profile is the same as for uniaxial flow, but the extension rate is always negative (compression), whereas for uniaxial flow it is always positive (tension). In *planar extension* one dimension of the material is extended while the second one is maintained constant and the third one compressed (Figure 6)^{1,2}.

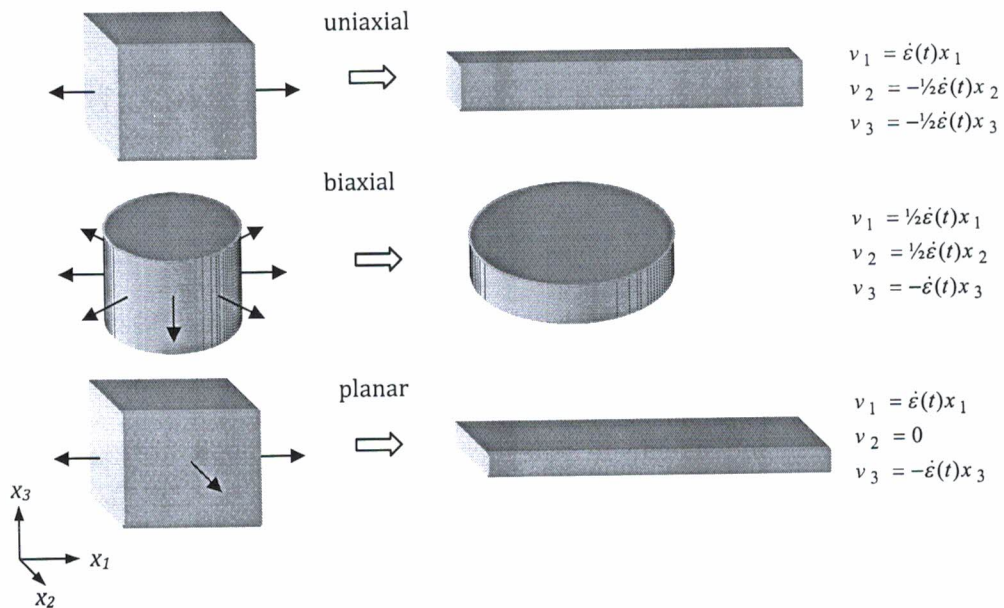


Figure 6. Uniaxial, planar, and biaxial extension and their velocity distributions

Typical curves of start-up test in uniaxial extension are given in Figure 7. Trouton's rule links shear and extensional properties together: in the linear region the curve should obey the *linear viscoelastic envelope* (LVE), which in uniaxial extension is three times the start-up shear viscosity η_s^+ when the shear rate is within the Newtonian flow region and viscosity thus independent of shear rate (Equation 23). In biaxial extension the multiplication factor is 6 (Equation 24), and in the planar case 4 in the x_1 direction and 2 in the x_2 direction (Equation 25).

$$\lim_{\dot{\epsilon}_H \rightarrow 0} |\eta_E^+(t, \dot{\epsilon}_H)| = 3\eta_s^+(t, \dot{\gamma} \rightarrow 0) \quad (23)$$

$$\lim_{\dot{\epsilon}_H \rightarrow 0} |\eta_B^+(t, \dot{\epsilon}_H)| = 6\eta_s^+(t, \dot{\gamma} \rightarrow 0) \quad (24)$$

$$\lim_{\dot{\epsilon}_H \rightarrow 0} |\eta_{P1}^+(t, \dot{\epsilon}_H)| = 4\eta_s^+(t, \dot{\gamma} \rightarrow 0) \quad (25)$$

$$\lim_{\dot{\epsilon}_H \rightarrow 0} |\eta_{P2}^+(t, \dot{\epsilon}_H)| = 2\eta_s^+(t, \dot{\gamma} \rightarrow 0) \quad (25)$$

Parameter $\dot{\epsilon}_H$ is the Hencky strain rate (logarithmic strain rate), which provides a correct measure of the strain rate when the deformation takes place in increments.

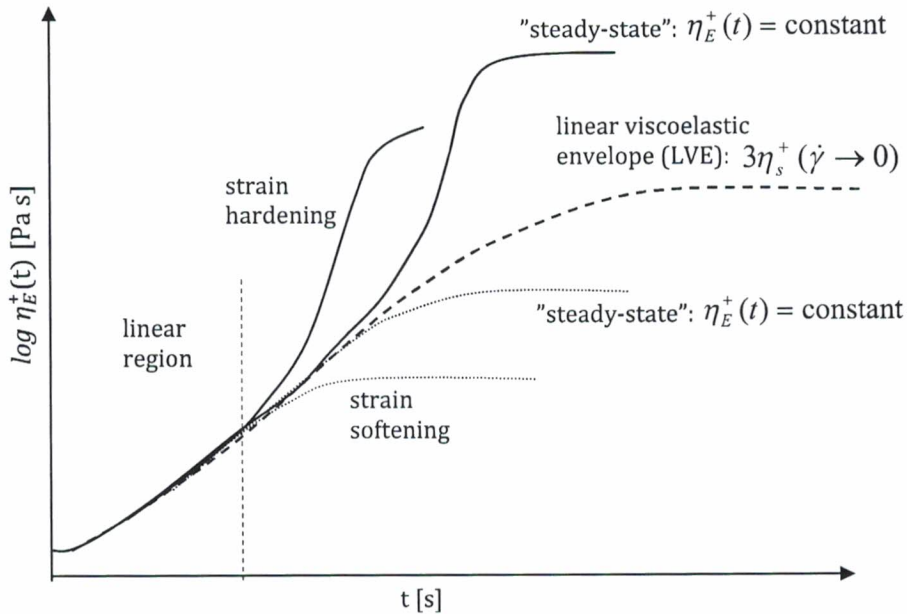


Figure 7. Start-up uniaxial extensional flow of polymer melts. Strain hardening behaviour is illustrated by solid lines and strain softening behaviour by dotted lines.

Non-linearity manifests itself as a deviation from the LVE: for *strain-hardening* materials the curves start to rise steeply before levelling off to a *steady-state*, where the viscosity becomes independent of time. For *strain-softening* materials the non-linearity appears as a steady-state level below the LVE. The steady-state flow may be difficult to observe in experiments, as instability of the sample and limitations of the test device often impair this.

Strong strain hardening in extensional flow is common for LCB polymers, and is attributed to the branched structure that efficiently constrains the flow: the steep rise in the start-up curve can be postulated to be caused by the stretching of the backbone between the branch points. Strain hardening can also be observed in linear polymers that have a bimodal MWD with small amount of very high- M_w fractions².

In most industrial melt processes the flow is a mixture of both elongational and shear flows: there is almost always stretching along the streamlines at some stage of the process. For example in injection molding, elongational flow occurs at gates and sudden changes in flow cross section where the melt accelerates, as well as at the front of the fountain-flow pattern in the cavity. Shearing is, however, a dominant deformation type in the mould cavity where the melt flows along the mold wall. Elongational flows dominate, for example, in film blowing, blow molding and fiber spinning processes, and in engineering of polymer resins for those applications the determination of extensional properties is crucial^{1,13}. Most often the extensional characterization is done in uniaxial extension, which most conveniently and effectively reveals strain hardening important

for processing methods involving extensional flow. Planar flow seems to mirror the uniaxial extension regarding the strain-hardening function, and biaxial flow behavior is closest to shear flow with only minor strain hardening¹³.

When the steady-state extensional viscosity values from start-up flow are plotted against Hencky strain rates, polymers with strong strain hardening in start-up flow typically exhibit a constant $\eta_E(\dot{\epsilon}_H)$, then *extension thickening* at increasing $\dot{\epsilon}_H$, followed by an *extension thinning* region in a similar manner to shear flow (Figure 8). However, not all strain hardening polymers necessarily have the extension thickening behavior over the same range of strain rates².

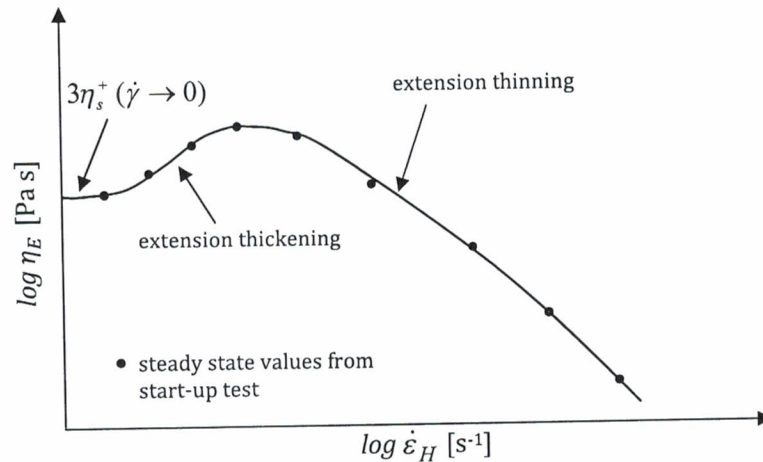


Figure 8. Typical curve of extensional viscosity vs. Hencky strain rate for an extension-thickening polymer

2.4 Viscosity models for shear-thinning polymer melts

Different models are used to describe the flow behavior of shear-thinning fluids. By fitting a model to the experimental data set, the flow behavior over wider than experimental range of shear rates can be predicted. The amount of free model parameters, as well as the models' predicting capability varies, some being more suitable e.g. for broad MWD polymers (gradual transition from Newtonian plateau to shear-thinning region) and some for narrow MWD polymers (sharp transition between Newtonian and shear-thinning regions). A typical shear viscosity curve for a polymer melt with different flow regions is presented in Figure 9, along with the parameters contributing to the fitting at each region.

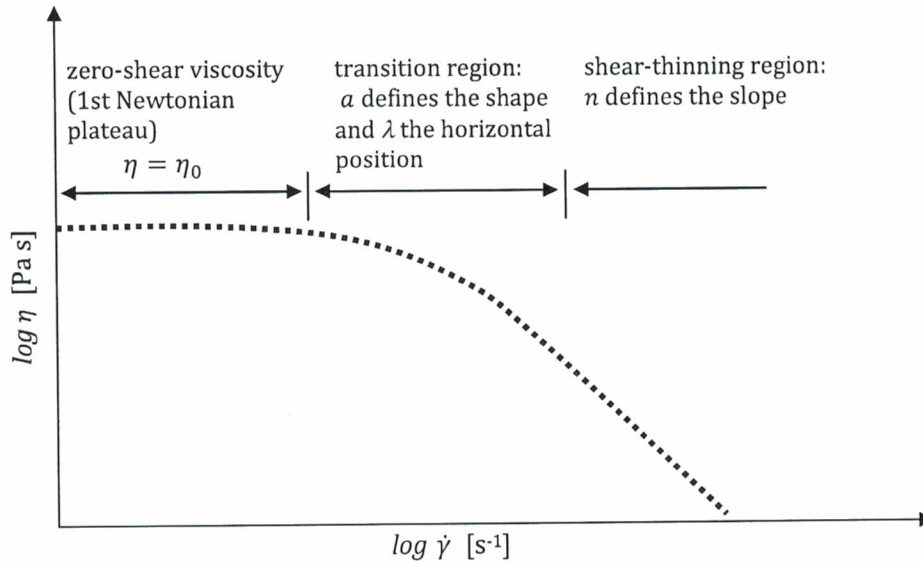


Figure 9. Typical shear viscosity curve for shear-thinning polymer melt

Power-Law -model (also: Ostwald - de Waele model) is the simplest viscosity model requiring two fitting parameters: K and n :

$$\eta(\dot{\gamma}) = K\dot{\gamma}^{n-1} \quad (26)$$

$n - 1$ is the slope of $\log \eta$ vs. $\log \dot{\gamma}$, thus for Newtonian materials $n = 1$, for shear-thinning material $n < 1$, and for shear-thickening materials $n > 1$. K relates to the magnitude of the viscosity being the vertical axis intercept on the \log viscosity vs. \log shear rate plot. The model is capable of describing either only Newtonian flow, or shear thinning (or shear thickening), and is thus of less use for polymer melts that show a Newtonian plateau at low shear rates and shear thinning at high shear rates. The Cross model is capable of describing Newtonian viscosity, shear-thinning viscosity, and also the transition area between them

$$\eta(\dot{\gamma}) = \frac{\eta_0}{1 + (\lambda\dot{\gamma})^{1-n}} \quad (27)$$

with fitting parameters: η_0 = zero-shear viscosity, n = power-law coefficient, and λ = characteristic time. For certain polymers a better fit at the transition area is achieved by the Carreau model

$$\eta(\dot{\gamma}) = \eta_0 [1 + (\lambda\dot{\gamma})^2]^{\frac{n-1}{2}} \quad (28)$$

Factor 2 in the exponents of the model makes the shift from zero-shear viscosity to Power-law area sharper. This model therefore describes best the viscosity function of narrow MWD polymers. The Carreau-Yasuda model has one freely adjustable parameter - a - more than the Cross and Carreau models, thus it is able to describe more gradual transition from Newtonian plateau to the shear-thinning region,

$$\eta(\dot{\gamma}) = \eta_0 [1 + (\lambda\dot{\gamma})^a]^{\frac{n-1}{a}} \quad (29)$$

therefore allowing a good fit also for polymers with broader MWD (long chain branched polymers). The Cross and Carreau models are actually only variations of the Carreau-Yasuda model, both having a fixed parameter for the curvature of the transient region

from Newtonian to shear-thinning behavior. For Cross model $a=1-n$, making the curvature dependent on the shear-thinning of viscosity, and for Carreau model $a=2$. The latter offers the least flexibility of these three models, and the fitting suits well only for polymers with sharp transition area, i.e. for polymers with relatively narrow MWD^{3,14}.

Temperature and pressure effects can be included in the fitting using a coefficient based either on the Arrhenius or WLF equation for temperature, and the Barus equation for pressure. Acknowledging both the temperature and pressure effect in the viscosity fitting is done by multiplying the individual shift factors a_T and a_p and including the total shift factor in the viscosity model, as for example here in the Carreau-Yasuda fitting:

$$\eta(\dot{\gamma}) = a_{T,p} \eta_0 \left[1 + (a_{T,p} \lambda \dot{\gamma})^a \right]^{\frac{n-1}{a}} \quad (30)$$

The viscosity models presented here are extensions of Newtonian constitutive equation (Equation 2) for viscous fluid flow. Unlike the Newtonian equation, they can also model the shear rate dependence of viscosity and are therefore called constitutive equations for *generalized Newtonian fluids* (GNF). Viscoelasticity, and thus for example the normal stress differences, cannot be described by GNF models³.

3 RHEOMETRY AND GOOD MEASUREMENT PRACTICE

Devices for shear rheology measurements can be roughly divided into drag-flow and pressure-flow based. Extensional properties can be measured using devices operating either in uniaxial, planar, or biaxial extension. Several types of devices for both shear and extensional flow exist, and only the ones used within this study are introduced in the following sections.

3.1 Cone-plate and parallel-plate rheometry

Drag flow can be generated, for example, by parallel-plate (plate-plate) or cone-plate geometries connected with rotational rheometers, which are commonly used for measuring the viscometric and viscoelastic functions of polymer melts. Drag flow between two rotating or oscillating plates is often called torsion flow due to the kinematics of the system. In the strain-rate controlled mode the deformation rate is set and the resulting torque recorded, and in the stress-controlled mode the torque is a pre-set value and the deformation is the measured quantity. Many rheometers are able to operate in both modes whereas some are limited to either stress or strain control. Only a very small sample amount is needed, and the tests can be run in either step-strain mode (shear rate profile from low to high rates or vice versa) or oscillatory (dynamic) mode. Rotational rheometers typically have very accurate temperature control in isothermal tests (convection oven used at $T > 200$ °C) and high torque resolution. The limitation of the function is usually set by the maximum deformation rates and stresses: flow instabilities, such as edge fracture (breakage of the sample layer between the plates) start to occur when the stress and strain become too high. Often the maximum shear rate in strain-rate controlled rheometers is less than 10 s^{-1} , but it varies by polymer depending also on the viscoelasticity of the sample⁵, and the gap at the rim (thus in case of cone-plate configuration, on the cone angle)¹⁵. The maximum measurable torque is commonly ~ 200 mNm which limits experimentation on high-viscous materials such as cross-linking rubbers or any polymer melt at very low temperature. The parallel-plate and cone-plate geometries are illustrated in Figure 10.

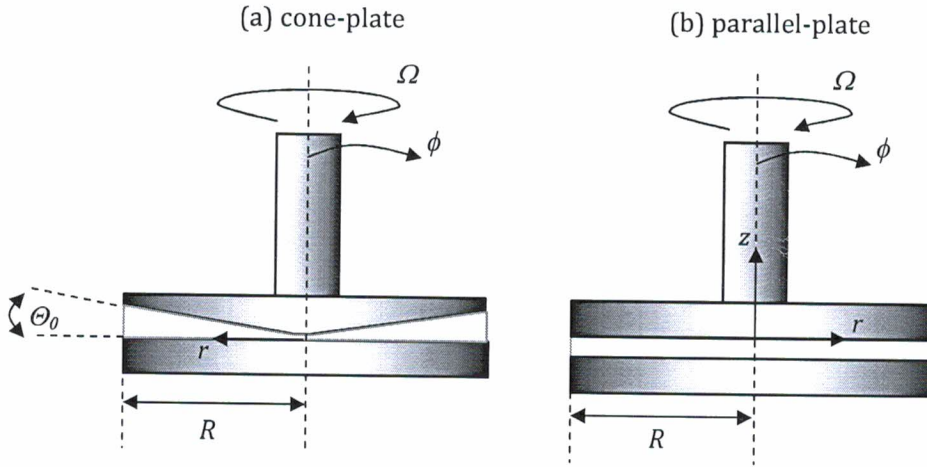


Figure 10. Principle of cone-plate and parallel-plate rheometer geometries

The cone-plate rheometer is the most popular device for measuring non-linear properties at small deformation rates. The upper part of the geometry has a conical profile with a truncated tip, which produces the uniform shear rate profile throughout the gap (Figure 10a). The gap between the cone and plate in the measurement position is determined by the imaginary tip of the cone, which would touch the lower plate. The shear rate is determined by angular velocity Ω and the angle between the cone and the plate Θ_0

$$\dot{\gamma} = \frac{\Omega}{\Theta_0} \quad (31)$$

The shear stress is

$$\tau = \frac{3M}{2\pi R^3} \quad (32)$$

and the shear viscosity thus

$$\eta = \frac{3M\Theta_0}{2\Omega\pi R^3} \quad (33)$$

The cone-plate system can also be used in dynamic (oscillatory) mode to measure linear viscoelastic properties. Then the SAOS functions are calculated as follows:

$$G'' = \frac{3\Theta_0 M_0 \sin \delta}{2\pi R^4 \phi_0} \quad (34)$$

$$G' = \frac{3\Theta_0 M_0 \cos \delta}{2\pi R^4 \phi_0} \quad (35)$$

where ϕ_0 is the angular amplitude of oscillation and M_0 is torque amplitude.

Shear rate in the parallel-plate system (Figure 10b) is determined by the angular velocity Ω , the thickness of the sample layer, i.e., gap between the plates, h , and the distance from the center of the plate r . Because of the rotation kinematics, the parallel-plate geometry produces an uneven velocity field: the shear rate is at highest on the rim and zero in the center of the plate. Shear rate at the rim is

$$\dot{\gamma}_R = \frac{R\Omega}{h} \quad (36)$$

and shear stress calculated from the measured torque M . When the geometry is used in rotational mode for measuring non-linear properties, a correction procedure must be applied in order to overcome the error caused by the non-constant shear rate profile. Then the shear stress has the form

$$\tau = \frac{2M}{\pi R^3} \left(\frac{3}{4} + \frac{1}{4} \frac{d \ln M}{d \ln \dot{\gamma}_R} \right) \quad (37)$$

where the term in brackets is the correction factor analogous to the Rabinowitsch correction, which is applied in capillary rheometry for true wall shear rate (see Chapter 3.2). Corrected viscosity is thus

$$\eta(\dot{\gamma}_R) = \frac{2M}{\dot{\gamma}_R \pi R^3} \left(\frac{3}{4} + \frac{1}{4} \frac{d \ln M}{d \ln \dot{\gamma}_R} \right) \quad (38)$$

For a Newtonian fluid the term in brackets yields 1 and shear viscosity is simply

$$\eta(\dot{\gamma}_R) = \frac{2M}{\dot{\gamma}_R \pi R^3} \quad (39)$$

In the dynamic operating mode in SAOS tests this problem is inexistent because of the minimal strain amplitude applied, and no correction is needed. In SAOS the storage- and loss moduli are determined as follows:

$$G'' = \frac{2hM_0 \sin \delta}{\pi R^4 \phi_0} \quad (40)$$

$$G' = \frac{2hM_0 \cos \delta}{\pi R^4 \phi_0} \quad (41)$$

From the moduli and the angular frequency, the complex viscosity can be calculated as shown in Equation 10.

Owing to the correction factor presented in Equation 37, the parallel-plate system can be used in the step-strain mode as well, although it is most commonly used for measuring the linear properties of the melts. Moreover, due to the non-constant shear field, the strain experienced by the fluid varies along the radius, and therefore for very strain-sensitive materials the result is a blur of all the strains measured. For such materials the cone-plate geometry may be a better option³.

3.2 Capillary rheometry

For the pressure-driven flow, capillary rheometers with round-hole or slit die geometry are commonly used. In this study the measurements were carried out using round-hole dies with different length to diameter ratios (L/D). Polymer granules are fed into the pre-heated rheometer barrel (Figure 11). After filling the barrel and reaching the thermal equilibrium, the melt is extruded through a capillary die at a defined piston speed and the melt pressure is recorded in the barrel above the die entrance or within the die. Using a round-hole die, usually having a radius from 0.5 to 1 mm, mounting a pressure transducer within the die is not possible, thus the pressure must be measured before the melt enters the capillary.

Calculation based on capillary flow involves some assumptions and simplifications¹⁵: (i) the flow is fully developed, steady, and isothermal, (ii) no slip at the capillary wall; fluid velocity at the wall is zero, and (iii) the fluid is incompressible and its viscosity independent of pressure. Actually not all of these assumptions always hold for non-Newtonian viscoelastic fluids. The invalid assumptions for fully developed flow and no-

slip at the capillary wall are handled by different corrections as will be discussed briefly in this chapter³.

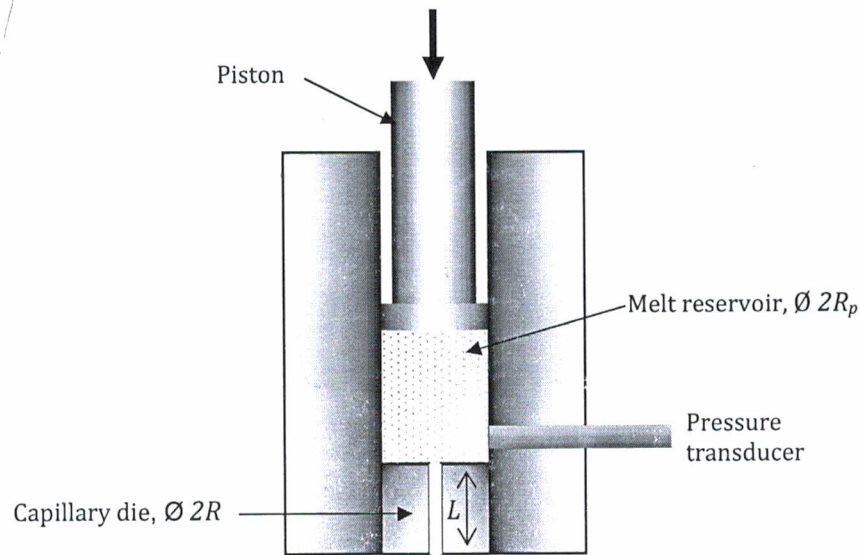


Figure 11. Principle of the capillary rheometer

The measurement is typically performed as a pre-set profile of alternating (either increasing or decreasing) shear rate. The volume flow rate in the barrel can be calculated as

$$Q = \pi R_p^2 V_p \quad (42)$$

where R_p is the barrel radius and V_p is the piston speed. From this and from the die dimensions the apparent shear rate, that is, the shear rate for a Newtonian fluid, at the capillary wall can be determined as

$$\dot{\gamma}_{wa} = \frac{4Q}{\pi R^3} \quad (43)$$

with R being the radius of the capillary. The apparent shear stress at the wall is calculated from the pressure (or actually from the difference between the atmospheric pressure and barrel pressure, Δp) measured in the barrel:

$$\tau_w = \frac{\Delta p}{2(L/R)} \quad (44)$$

For fluids with high molecular weight, elasticity causes disturbance of the flow pattern at the entrance of the capillary, where the fluid element stretches and accelerates through a sudden contraction. Similar effect, although much weaker, is observed at the die exit where the melt diverges. Re-circulating corner vortices have been observed in the entrance flow for some polymers, which has been related to a higher ratio of extensional to shear stress: the tendency to form a vortex increases with elasticity of the melt¹ (Figure 12).

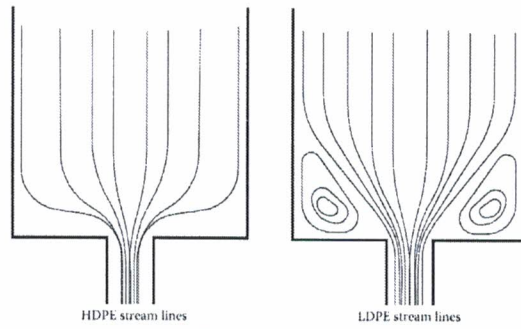


Figure 12. Melt stream lines in entrance flow at a contraction for a linear polymer (HDPE) and branched polymer (LDPE)¹⁶

Calculation in the capillary rheometry assumes a fully developed flow along the entire capillary length, thus omitting the end effects will lead to slightly overestimated pressure drop across the capillary. For achieving the true shear rate at the wall, τ_w , the extra pressure drop, Δp_e , arising at the entrance of the capillary die must be included in the calculation. The additional exit pressure drop at the capillary downstream is comparatively small and usually ignored. Correction is conventionally done through a Bagley correction procedure¹⁷: The measurements are repeated using at least three capillaries with the same diameter and different length. The Linear regression on the measured pressure vs. capillary L/D ratio plot is used to find the intersection on the pressure axis, which represents the pressure drop at the zero distance from the entrance, Δp_e (Figure 13).

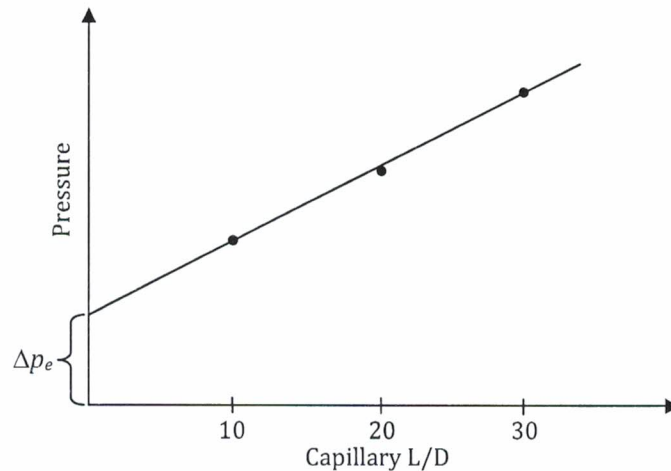


Figure 13. An example of Bagley plot with die length to diameter ratios 10, 20 and 30 at one measured shear rate.

For true wall shear stress the entrance pressure drop is subtracted from the total pressure drop across the capillary:

$$\tau_w = \frac{\Delta p - \Delta p_e}{2(L/R)} \quad (45)$$

A shortcut option for determining the entrance pressure drop is the use of an orifice die with a nominal length of zero. This procedure is discussed in detail and compared to the Bagley correction in Publication II.

A Newtonian, parabolic velocity profile in the capillary is assumed, although due to the shear thinning nature of polymer melts the profile is non-parabolic, resembling more a plug: the velocity is at highest in the centerline and zero at the wall, when the no-slip condition is valid. Thus the shear rate at the wall is at highest. The shape of the profile is defined by the power-law index n ; the smaller its value, the more the profile deviates from parabolic. Shear rate at the wall can be calculated using a procedure known as the Rabinowitsch or Weissenberg-Rabinowitsch correction:

$$\dot{\gamma}_w = \left(\frac{3n'+1}{4n'} \right) \dot{\gamma}_{wa} \quad (46)$$

The local power-law index n' at each shear rate for any fluid is obtained by numerical derivation as a slope of the apparent shear rate vs. wall shear stress on a double logarithmic plot:

$$n' = \frac{d \log \tau_w}{d \log \dot{\gamma}_{wa}} \quad (47)$$

The most straightforward way of performing the Rabinowitsch correction for experimental data is through a polynomial fitting on $\log \tau_w$ vs. $\log \dot{\gamma}_{wa}$. Differentiation of the polynomial equation in terms of each $\log \dot{\gamma}_{wa}$, gives the local power law index n' for each measured shear rate. For power-law fluids the slope of the polynomial fitting curve remains constant, thus $n' = n$. Viscosity corrected for both entrance pressure drop and the non-Newtonian flow profile is then

$$\eta = \frac{\tau_w}{\dot{\gamma}_w} = \frac{R(\Delta p - \Delta p_e)}{2L[(3n'+1)/4n']\dot{\gamma}_{wa}} \quad (48)$$

Correction for the entrance pressure drop and plug-like flow in pressure-driven contraction flow are well-known procedures in capillary rheometry. Nevertheless, their significance is sometimes overlooked and the data handling phase skipped. This can perhaps be justified for quality-control purposes where the only goal is to ensure the consistence of a polymer grade between different polymerization batches, and the control is done comparing the test results obtained for different batches always using an identical test procedure. When the aim is to examine the true rheological behavior of polymers and the reflections of molecule-level properties, such as chain architecture or molecular weight distribution to the rheology, it becomes extremely important to follow careful experimental procedures minimizing the influence of all external factors, and also to perform all the possible corrections that eliminate the errors caused by the above discussed assumptions. This is equally important when measured data is used for process simulation purposes: the models for flow simulation give good predictions only if the measured data used to form the data bank for each material is exact and correct.

The general no-slip assumption of classical fluid mechanics dictates that the melt adheres to the capillary or slit wall. However, for some polymers, when a critical shear stress is exceeded, the melt starts to slip along the wall, thus the fluid velocity at the capillary wall is nonzero and the true shear rate smaller than in a no-slip case. The wall slip can be determined by performing parallel measurements with dies having a different diameter but the same length-to-diameter (or radius) ratio: if the plot of apparent shear rate vs. $1/R$ at constant wall shear stress gives a horizontal line, no slip occurs. If the curve is linear with a positive slope, slip occurs, and the slip velocity at the wall can be calculated from the slope, according to the procedure proposed by Mooney¹⁸.

Entrance pressure drop in capillary rheometer with either round-hole or slit die can be used to evaluate the extensional viscosity. Contraction flow analysis method is based on the assumption, that the pressure drops due to shear and extensional deformation

can be calculated separately and their sum is the total pressure drop. Additionally the general assumptions of capillary rheometry are applied in the contraction flow analysis as well. Cogswell¹⁹ and Binding²⁰ analyses are the most popular techniques for estimating the extensional viscosity from the capillary rheometry data. The first one is discussed in more detail and compared to extensional viscosity in uniaxial extension in Publication IV.

3.3 Slit rheometry

Instead of a round-hole capillary, a wide $w \times h$ slit can also be mounted on a capillary rheometer to measure rheological properties in pressure-driven flow (Figure 14). The calculation presumes that the slit is infinitely wide, which in practice can be assumed with a good accuracy when $w \geq 10h$. When this is the case, the effect of the edges can be ignored. The main advantage of a slit die is its flat wall geometry that enables measurement of pressure directly in the slit where the flow is fully developed, thus making exact determination of pressure profile possible. For this reason, the correction of the entrance pressure drop is unnecessary. Slit dies are, however, more difficult to assemble and to disassemble. In addition, cleaning of the slit edges requires more effort: possible remnants of burned or charred melt at the edges can reduce the die dimensions and thus cause a computational error²¹. Another source of error possibly occurring with a slit die is the so called hole-pressure error, related to the normal forces present in the flow of viscoelastic fluids over a discontinuity of the pressure transducer bore. Slit constructions and hole pressure error can also be used for determining the normal stress differences by means of transverse pressure transducer: the hole-pressure error can roughly be approximated to be one third of the first normal stress difference for shear-thinning fluids²².

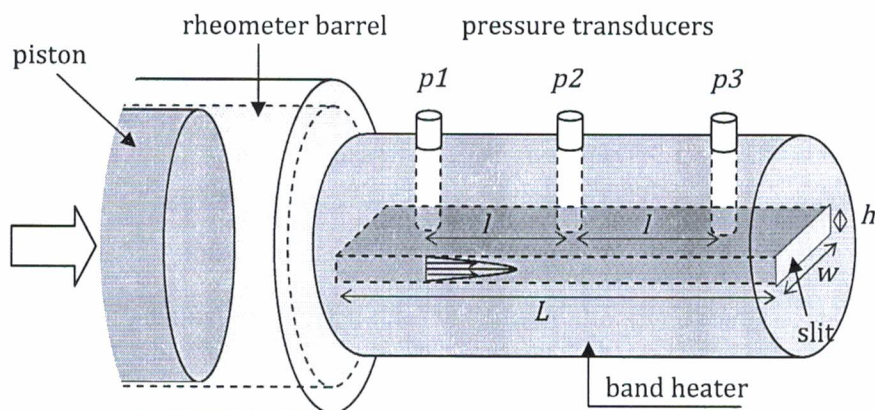


Figure 14. An illustrational drawing of a slit die rheometer

Shear stress on the slit wall is

$$\tau_w = \frac{h \Delta p}{2 l} \quad (49)$$

where $\Delta p = p_1 - p_2 = p_2 - p_3$ if the pressure profile is linear, that is, if neither pressure dependent viscosity nor viscous heating cause any curvature to the pressure

profile across the slit. In capillary geometry these possible non-linearities can be observed as an upward (pressure dependence) or downward (viscous heating) curvature of the Bagley plot for end corrections^{22,23}. The shear rate for a Newtonian fluid (apparent shear rate) in a rectangular slit is

$$\dot{\gamma}_{wa} = \frac{6Q}{h^2w} \quad (50)$$

For shear-thinning polymers the correction for the non-parabolic velocity profile must be performed analogously to the Rabinowitsch correction for capillary die calculations:

$$\dot{\gamma}_w = \frac{6Q}{h^2w} \left(\frac{2n'+1}{3n'} \right) \quad (51)$$

where

$$n' = \frac{d \log \tau_w}{d \log \dot{\gamma}_{wa}} \quad (52)$$

Shear viscosity at the slit wall is then

$$\eta = \frac{\tau_w}{\dot{\gamma}_w} = \frac{h\Delta p}{2l[(2n'+1)/3n']\dot{\gamma}_{wa}} \quad (53)$$

A simpler, yet reasonably accurate alternative for accounting for the non-Newtonian velocity profile has been proposed by Schümmer and co-workers^{24,25}, and developed further by Giesekus and Langer²⁶. This procedure is based on estimating the shear rate and viscosity at radial distance r (for circular geometry) or vertical distance y from the flow slit center (for a rectangular slit), where the apparent shear rate equals the true shear rate. Hence, considering that under fully developed conditions the apparent shear rate, as well as the shear stress, varies linearly with radial position, one obtains

$$\eta(x^*\dot{\gamma}_{wa}) = \eta_a(\dot{\gamma}_{wa}) \quad (54)$$

Factor $x^* = r/R$ for a circular capillary, where R = radius of the die, and for a slit geometry $x^* = 2y/h$, where h is the slit height²⁶. Apparently, when $n = 0.36 - 1.2$, x^* varies by only a small amount, so that a representative value of x^* may be chosen for most materials with very little loss in accuracy. For rectangular slit this approximation is given as¹

$$x^* = \left(\frac{2n+1}{3n} \right)^{n/(n-1)} \approx 0.79 \quad (55)$$

and for circular capillary as

$$x^* = \left(\frac{3n+1}{4n} \right)^{n/(n-1)} \approx 0.83 \quad (56)$$

The Schümmer approximation is valid for a true shear stress $\gamma^* \tau_w$. It shifts data only horizontally (to the left) and can be applied to single points.

3.4 Rheological measurements with polymer processing machines

In order to achieve data at high shear rates relevant for injection molding, performing rheological measurement using a capillary or slit die connected to an injection molding machine is an attractive option. This way the measurable melt experiences similar thermal and shear history as in actual processing, and thus the results from such measurements can be assumed to best serve for the evaluation of processability of a polymer. Moreover, use of processing machines as rheometers often enables achieving higher deformation rates which are out of the measurement range of a regular capillary rheometer.

Continuous in-process experiments can be separated by means of the melt flow through the measurement device: In in-line measurements the entire melt stream passes through the measurement unit. By-pass on-line experiments are referred to, when the measurement is only made for a part of the melt stream that is directed to by-pass the process stream through the meter. In recycled on-line measurement, the by-passed melt stream is directed back to the process line after measurement²⁷. In many works where the plasticizing is done by an injection molding machine and the pressures are recorded in the die fixed on the mounting table, the term “in-line measurement” is used^{28,29}. One can, however, also understand the in-line measurement as an experiment that is carried out simultaneously with actual processing. In the case where a slit or capillary die is mounted to an injection molding machine, it replaces the mold, thus no actual molding can be done at the same time with such experiments and the term “in-line” must be understood a bit differently.

Rheological measurements can be accomplished by means of a die, either circular or rectangular, where the pressure and temperature are recorded by transducers mounted on the die wall and/ or entrance. Such a measurement unit can be connected to either an extruder or an injection molding machine. In case of extrusion, continuous screw rotation causes the flow through the die, and therefore the flow rate cannot be calculated simply from the screw rotation speed and barrel dimensions, but the characteristic flow resistance of the die has to be considered as well¹. The accurate flow rate can be determined by collecting the extrudate over a specified time period, weighing it, and using the melt density value of the material to convert the mass-flow rate to volume-flow rate²⁷. After this the shear rate corresponding to the screw rotation speed can be calculated. In an injection molding machine the calculation of the flow rate is more straightforward; injection through the die occurs shot-wise by a rapid movement of the screw at a pre-determined speed and over a set distance, and the flow rate can be calculated using Equation 42. However, especially at low injection pressure, one has to consider the possible leakage flow of melt from the nozzle, backwards along the screw, which can reduce the theoretical flow rate³⁰.

High shear-rate viscosity has been examined by circular capillary die specially designed and built in-house^{31,32,33}. Tailor-made rectangular slit dies and hyperbolically converging and diverging planar dies have also been used for extensive examination of shear and elongational properties of polymers³⁴ utilizing Cogswell and Binding analyses for determining the apparent extensional properties. At the moment a commercial device with a wide slit³⁰ compatible with injection molding machine also exists. The slit die experiments using an injection molding machine as a rheometer are discussed further in Publication VI.